Spine Deformity

www.spine-deformity.org

Spine Deformity 5 (2017) 37–45

Computed Tomography Study

Asymmetry of the Vertebral Body and Pedicles in the True Transverse Plane in Adolescent Idiopathic Scoliosis: A CT-Based Study

Rob C. Brink, MD[a], Tom P.C. Schlösser, MD, PhD[a], Dino Colo, MD[a], Koen L. Vincken, PhD[b], Marijn van Stralen, PhD[c], Steve C.N. Hui, MSc[d], Winnie C.W. Chu, MD, FRCR[d], Jack C.Y. Cheng, MD, FRCSEd[e], René M. Castelein, MD, PhD[a,*]

[a]*Department of Orthopaedic Surgery, University Medical Center Utrecht, Utrecht, The Netherlands*
[b]*Image Sciences Institute, University Medical Center Utrecht, Utrecht, The Netherlands*
[c]*Imaging Division, University Medical Center Utrecht, Utrecht, The Netherlands*
[d]*Department of Imaging & Interventional Radiology, Prince of Wales Hospital, The Chinese University of Hong Kong, Shatin, Hong Kong*
[e]*Department of Orthopaedics and Traumatology, Prince of Wales Hospital, The Chinese University of Hong Kong, Shatin, Hong Kong*

Received 27 June 2016; accepted 10 August 2016

Abstract

Study Design: Cross-sectional.
Objectives: To quantify the asymmetry of the vertebral bodies and pedicles in the true transverse plane in adolescent idiopathic scoliosis (AIS) and to compare this with normal anatomy.
Summary of background data: There is an ongoing debate about the existence and magnitude of the vertebral body and pedicle asymmetry in AIS and whether this is an expression of a primary growth disturbance, or secondary to asymmetrical loading.
Methods: Vertebral body asymmetry, defined as left-right overlap of the vertebral endplates (ie, 100%: perfect symmetry, 0%: complete asymmetry) was evaluated in the true transverse plane on CT scans of 77 AIS patients and 32 non-scoliotic controls. Additionally, the pedicle width, length, and angle and the length of the ideal screw trajectory were calculated.
Results: Scoliotic vertebrae were on average more asymmetric than controls (thoracic: AIS 96.0% vs. controls 96.4%; $p = .005$, lumbar: 95.8% vs. 97.2%; $p < .001$) and more pronounced around the thoracic apex (95.8%) than at the end vertebrae (96.3%; $p = .031$). In the thoracic apex; the concave pedicle was thinner (4.5 vs. 5.4 mm; $p < .001$) and longer (20.9 vs. 17.9 mm; $p < .001$), the length of the ideal screw trajectory was longer (43.0 vs. 37.3 mm; $p < .001$), and the transverse pedicle angle was greater (12.3° vs. 5.7°; $p < .001$) than the convex one. The axial rotation showed no clear correlation with the asymmetry.
Conclusions: Even in non-scoliotic controls is a degree of vertebral body and pedicle asymmetry, but scoliotic vertebrae showed slightly more asymmetry, mostly around the thoracic apex. In contrast to the existing literature, there is no major asymmetry in the true transverse plane in AIS and no uniform relation between the axial rotation and vertebral asymmetry could be observed in these moderate to severe patients, suggesting that asymmetrical vertebral growth does not initiate rotation, but rather follows it as a secondary phenomenon.
Level of Evidence: Level 4.

Keywords: Adolescent idiopathic scoliosis; Transverse plane morphology; Axial rotation; Vertebral body asymmetry; Pedicle asymmetry; CT scan

Abbreviations: 3-D, three-dimensional; AIS, adolescent idiopathic scoliosis; CT, computed tomographic; ICC, intraclass correlation coefficients; MANOVA, multiple analysis of variances; NCJ, Neurocentral junctions; r, Pearson correlation coefficient.

IRB approval: This study was reviewed and approved by the Medical Ethics Review Committee of the University Medical Center Utrecht.

Author disclosures: RCB (none); TPCS (none); DC (none); KLV (none); MvS (none); SCNH (none); WCWC (none); JCYC (none); RMC (grants from Alexandre Suerman UMC Utrecht PhD grant, grants from K2M research grant, grants from Medtronic research grant, outside the submitted work).

*Corresponding author. Department of Orthopedic Surgery, University Medical Center Utrecht, G05.228, P. O. Box 85500, 3508 GA Utrecht, The Netherlands. Tel.: +31887554578; fax: +31302510638.

E-mail address: R.M.Castelein@umcutrecht.nl (R.M. Castelein).

2212-134X/$ - see front matter © 2016 Scoliosis Research Society. All rights reserved.
http://dx.doi.org/10.1016/j.jspd.2016.08.006

Introduction

Transverse plane asymmetry is a well-known part of the three-dimensional (3-D) deformity in scoliosis and has been described in a number of older as well as more recent anatomic and radiographic imaging studies [1-8]. Unfortunately, these data are sometimes inconsistent and conflicting, describing scoliosis of different origin and age at onset of deformity. The exact transverse plane morphology in adolescent idiopathic scoliosis (AIS) is important, because it may further our understanding of the true nature of the disorder and its etio-pathogenesis. It is known that all growth cartilage of the pedicles, the neurocentral junctions (NCJs), close before the age of eight; therefore, pronounced pedicle asymmetry suggests a disturbance of symmetrical development that has started already before that age [9]. Furthermore, for surgical strategy, the exact morphology of both vertebral body and pedicles is important as a reference for pedicle screw orientation, length, and width [8,10-15]. In addition to the existing literature on pedicle asymmetry in AIS, this study aims to determine the existence and magnitude of vertebral body and pedicle morphology asymmetry in the true transverse plane in patients with moderate to severe AIS.

Materials and Methods

Study population

All AIS patients who had received preoperative high-resolution computed tomographic (CT) images (64 Slice Multi-detector CT scanner; GE Healthcare, Chalfont, St. Giles, United Kingdom; slice thickness 0.625 mm)—acquired for navigation-guided pedicle screw insertion in one of the participating centers—between June 2011 and May 2013 were included. All patients had undergone routine upright posterior-anterior and bending radiography and supine magnetic resonance imaging of the full spine for detection of spinal cord abnormalities. Children with other spinal pathology, spinal trauma, previous spinal surgery, neurological symptoms or neural axis abnormalities, syndromes associated with disorders of growth, or atypical left convex thoracic curves or right convex (thoraco) lumbar curves were excluded to obtain an as homogeneous population as possible. Hence, the right pedicle is always the convex pedicle and the left pedicle the concave pedicle in this study. The control group consisted of 32 sex-matched nonscoliotic subjects who had undergone CT imaging of the thorax and abdomen for indications other than spinal pathology.

Computed tomographic measurement method

Vertebral body and pedicle asymmetry were measured for each individual vertebra by two trained observers (R.B. and T.S.), using in-house–developed software for semi-automatic analysis (ScoliosisAnalysis, Image Sciences Institute, Utrecht, The Netherlands), based on MeVisLab (MeVis Medical Solutions AG, Bremen, Germany) [16]. For intra- and interobserver reliability, two observers (R.B. twice, T.S. once) analyzed a random subset of 10 CT scans of AIS patients on separate sittings.

First, the observer selected the upper and lower endplates of the vertebral body, by using the software that was developed for this purpose [16]. Then, the observer used the sagittal and coronal orientation of the endplates to correct for coronal and sagittal tilt to position each vertebral level in the true transverse plane. Subsequently, for each endplate, its longitudinal axis was calculated automatically

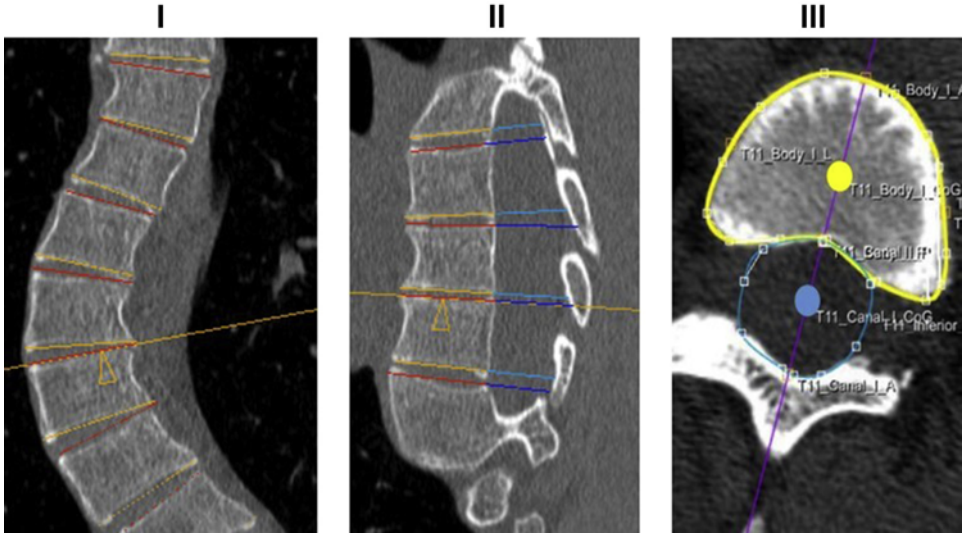

Fig. 1. The orientation of the upper and lower endplate of each individual vertebra of the computed tomography scans was determined by using the semi-automatic software, correcting for coronal (I) and sagittal (II) tilt, to reconstruct true transverse sections. The observer drew a contour around the vertebral body (yellow line in III) and spinal canal (blue line in III). The semiautomatic software calculated a center of gravity of the vertebral body (yellow dot in III) and spinal canal (blue dot in III). For each endplate, its longitudinal axis was calculated as the line between those two points (purple line in III).

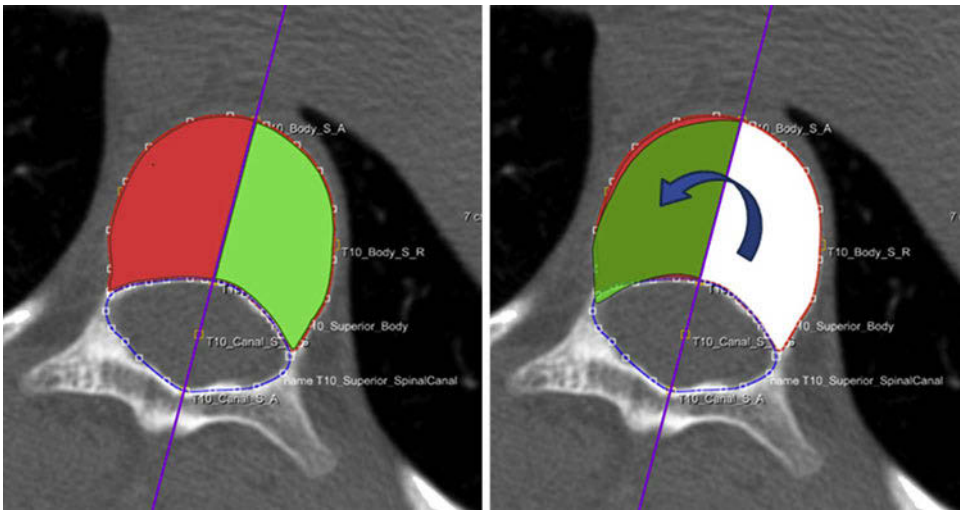

Fig. 2. Computed tomographic images showing the true transverse reconstructions of a vertebra. After manual segmentation of the vertebral body and spinal canal, the software flipped the right side of the endplate across the longitudinal vertebral axis. The Dice similarity coefficient was used to calculate the percentage of overlap between the left (in *green*) and right (in *red*) side of the vertebral body.

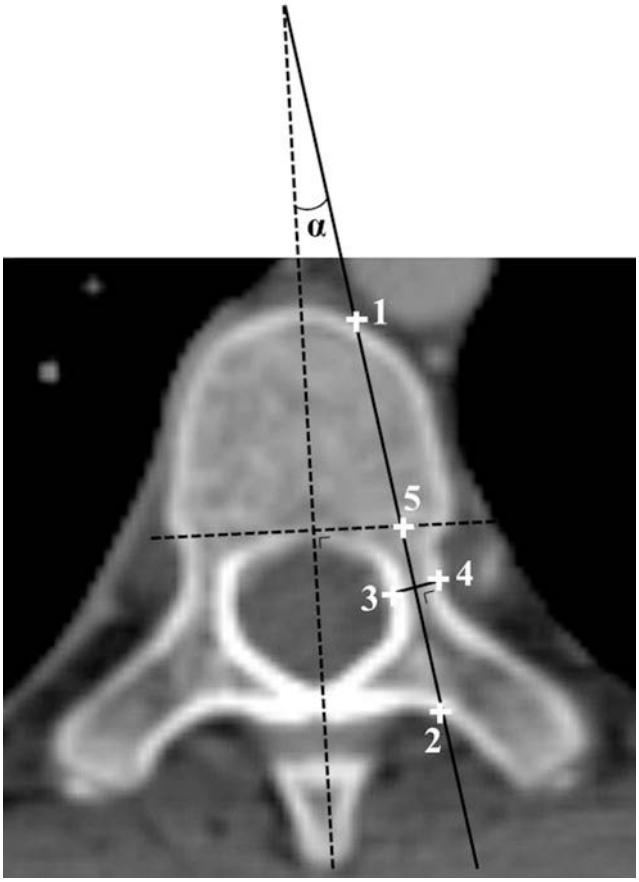

Fig. 3. Pedicle width was defined as the narrowest length between the medial outer cortex and lateral outer cortex on the right–left axis (point 3–4); pedicle length as the length between the posterior outer cortex of the lamina and the anterior side of the spinal canal on the longitudinal axis (2–5); length of the ideal pedicle screw trajectory as the length between the posterior outer cortex and the anterior outer cortex of the vertebral body on the longitudinal axis (1–2; mimicking the length of the ideal pedicle screw trajectory in the transverse plane) and the transverse pedicle angle as the angle between the pedicle axis and the vertebral axis (α).

after manual segmentation (Fig. 1) [16]. Axial rotation of each vertebra was calculated, using the 3-D orientation of the longitudinal axis of the endplates as relative to the sacrum, since this normally is not rotated in AIS [16]. For measuring the vertebral body asymmetry, the right side of the endplate of the vertebral body was flipped across the longitudinal axis on top of the left side to calculate the overlap between them using the Dice similarity coefficient; that is, 100% indicates perfect symmetry, 0% complete asymmetry (Fig. 2).

Pedicle asymmetry was also analyzed in the ideal reconstructed transverse sections, parallel to the upper endplate, on which both pedicles were best visible, as previously used by other research groups for pedicle asymmetry analyses [11,17]. A longitudinal line was placed straight through each pedicle, the pedicle axis, and perpendicular to this axis, a right–left axis was reconstructed. The pedicle width and length, length of the ideal screw trajectory and the pedicle angle were measured by using these axes, specified in Fig. 3. Pedicle asymmetry was defined as the difference between the convex and concave pedicle.

For better comparison with previous studies on pedicle asymmetry, pedicles were also classified as proposed by Watanabe et al. and Sarwahi et al. [13,18]. This classification describes four pedicle types; type A, a cancellous channel >4 mm; type B, a cancellous channel between 2 and 4 mm; type C, a cortical channel >2 mm; and type D, a cancellous or cortical channel <2 mm.

Statistical analysis

Statistical analyses were performed using SPSS 20.0 for Windows (SPSS Inc., Chicago, IL). Descriptive statistics

were computed and chi-square was used to analyze the differences in pedicle classification. Potential outliers were identified. Differences in vertebral body and pedicle parameters between AIS patients and controls were analyzed, using multiple analysis of variances (MANOVA). In addition, paired t-tests were used to analyze the parameters between the concave and convex side, and between the apices and Cobb end vertebrae in the AIS group. Pearson's correlation coefficient (r) was used to define the relationship between the asymmetry and axial rotation, and the intraclass correlation coefficient (ICC) was used to define the intra- and interobserver reliability. The statistical significance level was set at 0.05.

Results

Population

Seventy-seven AIS patients were included, only the vertebrae of the primary structural thoracic (Lenke 1, 2, 3, and 4) and lumbar (Lenke 5 and 6) curves in AIS were included (see Table 1 for exclusion criteria and demographics). To assess potential confounding of the different age of the groups, the effect of age on outcome was analyzed, which showed no difference ($p \geqslant .147$).

Table 1
Demographics for all included subjects and exclusion criteria are shown.

Included	AIS (n = 77)	Controls (n = 32)
Age (y)		
Range	11–26	10–18
Mean ± SD	17.1 ± 2.9	15.4 ± 1.8
Girls, n (%)	60 (78%)	25 (78.1%)
Thoracic curve convexity, n (%)		
Right convex	77 (100%)	
Lenke curve type		
I	37 (48%)	
II	16 (21%)	
III	7 (9%)	
IV	2 (3%)	
V	6 (8%)	
VI	9 (12%)	
Primary thoracic curves	62 (81%)	
Cobb angle primary thoracic curve (°)		
Range	51–105	
Mean ± SD	69 ± 12	
Primary lumbar curves	15 (19%)	
Cobb angle (thoraco) lumbar curve (°)		
Range	41–88	
Mean ± SD	41 ± 16	
Excluded, n		
Total	11	
Associated congenital of neuromuscular pathologies	6	
Atypical left convex thoracic curve	3	
Scoliosis surgery prior to CT scan	1	
Incomplete radiological chart	1	

AIS, adolescent idiopathic scoliosis; CT, computed tomography; SD, standard deviation.

Curve characteristics (curve type according to the Lenke classification, level of the apex, and Cobb angles) were determined on the conventional posterior-anterior and bending radiographs [19-21].

Overall asymmetry between AIS and controls

Primary thoracic and lumbar AIS curves had on average, considering the mean of all the vertebrae in the curve, more transverse plane asymmetry than controls in terms of vertebral body asymmetry (thoracic, 96.0% ± 0.6% in AIS vs. 96.4% ± 0.5% in controls, $p = .005$; lumbar, 95.8% ± 1.2% vs. 97.2% ± 0.4%, $p < .001$; Fig. 4).

Pedicle width: the AIS concave pedicle was thinner than the convex pedicle (thoracic, −0.4 ± 0.6 mm left–right difference in AIS vs. 0.1 ± 0.3 mm left–right difference in controls, $p < .001$; lumbar, 0.5 ± 0.7 mm vs. 0.2 ± 0.3 mm, $p = .036$; Fig. 5). All the included curves were right convex; therefore, the right pedicle is the convex pedicle and the left pedicle is the concave pedicle.

The concave pedicle was longer in the thoracic spine as compared to the convex pedicle (1.8 ± 1.7 mm left–right difference in AIS vs. 0.7 ± 0.8 mm in controls; $p < .001$; lumbar, −0.9 ± 1.2 mm vs. −0.3 ± 1.2 mm; $p = .09$; Fig. 5).

Length of the ideal screw trajectory in the thoracic spine: the AIS concave pedicle was longer (4.1 ± 2.3 mm left–right difference in AIS vs. 1.2 ± 1.0 mm in controls; $p < .001$). In the lumbar spine the length of the ideal pedicle screw trajectory showed, somewhat surprisingly, more asymmetry in the controls (0.9 ± 1.5 mm) than in AIS patients (−0.2 ± 1.3 mm; $p = .015$; Fig. 5).

The AIS concave pedicle was more angled inward (throacic, 4.6° ± 3.2° left–right difference in AIS vs. 1.8°

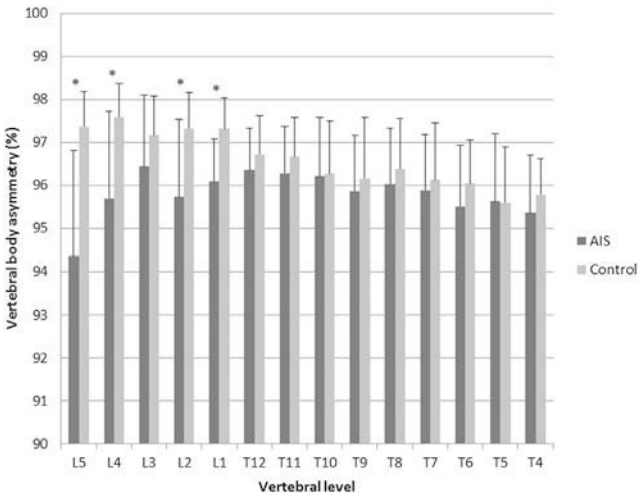

Fig. 4. The vertebral asymmetry is shown for each individual vertebral level in the primary thoracic and primary lumbar curve in adolescent idiopathic scoliosis (AIS) and the thoracic and lumbar vertebrae in controls. 100% indicates perfect symmetry, 0% complete asymmetry. *Significant difference between AIS and controls.

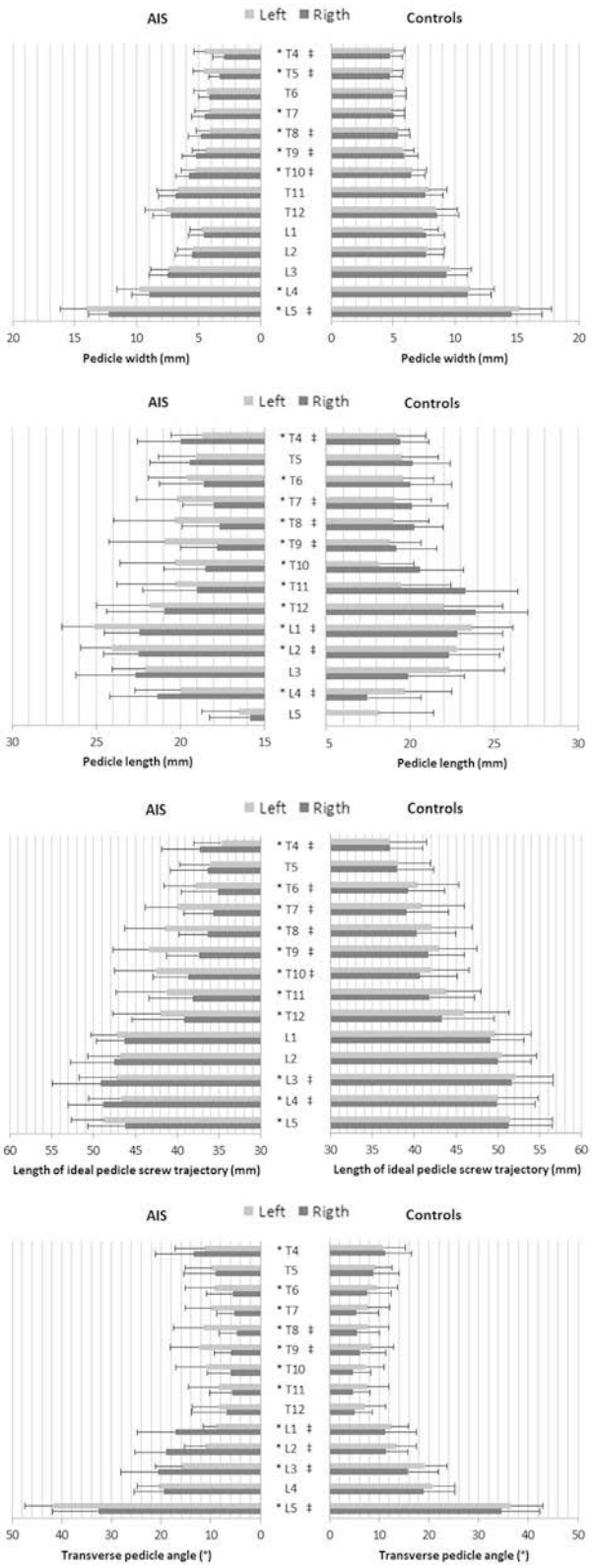

Fig. 5. Pedicle asymmetry is shown for each individual pedicle in adolescent idiopathic scoliosis (AIS) patients and controls, representing pedicle width, pedicle length, the length of the ideal pedicle screw trajectory, and the transverse pedicle angle. The right pedicle is the convex pedicle in the primary thoracic AIS curves and the concave in the primary lumbar, the left pedicle is the concave in the primary thoracic curves and the convex in primary lumbar curves. *Significant difference between concave and convex pedicle in AIS patients; ‡Significant difference in asymmetry (difference between right and left pedicle) between AIS patients and controls.

± 2.1° in controls, $p < .001$; lumbar, −4.7° ± 4.0° vs. 2.2° ± 3.3°, $p < .001$; Fig. 5).

Overall asymmetry between concave and convex pedicle in AIS

On average, throughout the thoracic primary curves, the concave pedicle was thinner (concave 5.2 ± 1.0 mm vs. convex 5.6 ± 0.9 mm; $p < .001$) and longer (concave 20.6 ± 2.0 mm, convex 18.8 ± 1.8 mm; $p < .001$), the ideal screw trajectory was also longer (concave 41.7 ± 3.6 mm vs. convex 37.6 ± 3.6 mm; $p < .001$) and the transverse pedicle angle was greater (concave 10.6° ± 3.6° vs. convex 6.0° ± 3.0°; $p < .001$). In the primary lumbar curves, the concave pedicle was thinner (concave 6.9 ± 1.1 mm vs. convex 7.4 ± 1.2 mm; $p = .018$), but slightly shorter (concave 21.6 ± 1.6 mm vs. convex 22.5 ± 1.4 mm; $p = .009$) and the transverse pedicle angle was also greater (concave 18.0° ± 4.7° vs. convex 13.3° ± 3.9°; $p < .001$). There was on average no significant difference between concave (46.5 ± 3.4 mm) and convex (46.3 ± 3.2 mm) regarding length of the ideal screw trajectory in the primary lumbar curves. The pedicles in the controls showed no asymmetry between the left and right pedicle for all the parameters ($p \geq .051$).

Pedicle type asymmetry

In the primary thoracic AIS curves, 20.3% of the pedicles were abnormal—type B, C, or D—compared to only 7.8% in the corresponding vertebrae in the controls ($p < .001$; Table 2). In the primary lumbar curves, 7.7% of the pedicles were abnormal, versus 0.0% in the controls ($p < .001$). The concave pedicle in the thoracic AIS curve was more often type B (concave 18% vs. convex 12%; $p = .016$) or type C (concave 8% vs. convex 2%; $p < .001$; Table 2) than the convex pedicle. In the lumbar AIS curve, there was no difference between the concave and convex pedicle.

Vertebral body and pedicle asymmetry in different regions of the spine

The thoracic apical vertebrae of the primary curves showed more asymmetry than the end vertebrae (often also the neutral

Table 2
The pedicle classification is shown for the thoracic and lumbar primary curves in AIS patients and compared to the corresponding vertebrae in the controls.

Pedicle type	Thoracic				Lumbar			
	Convex, n (%)	Concave, n (%)	p	Controls, n (%)	Convex, n (%)	Concave, n (%)	p	Controls, n (%)
A	353 (86)	304 (74)	<.001	649 (92)[a]	74 (95)	70 (90)	.184	448 (100)[a]
B	51 (12)	74 (18)	.016	36 (5)[a]	2 (3)	4 (5)	.341	0 (0)[a]
C	8 (2)	33 (8)	<.001	19 (3)[a]	2 (3)	4 (5)	.341	0 (0)[a]
D	0 (0)	1 (0)	.500	0 (0)	0 (0)	0 (0)	—	0 (0)

AIS, adolescent idiopathic scoliosis.

Type A = cancellous channel >4 mm; type B = cancellous channel between 2 and 4 mm; type C = cortical channel >2 mm; type D = cancellous or cortical channel <2 mm.

[a] Significant difference between AIS and controls.

vertebrae) in left–right overlap (apex, 95.8 ± 1.5% vs. end vertebra, 96.3 ± 1.0%; p = .031), the difference between convex and concave pedicle width (0.9 ± 1.1 mm vs. −0.2 ± 1.1 mm; p < .001), pedicle length (−3.0 ± 3.8 mm vs. −0.5 ± 2.7 mm; p < .001), length of the ideal screw trajectory (−5.7 ± 5.2 mm vs. −2.0 ± 4.1 mm, p < .001) and transverse pedicle angle (−6.6° ± 6.8° vs. −1.7° ± 7.4°; p < .001; Fig. 6). In the lumbar spine, no significant difference in asymmetry was found between the apical and end vertebrae.

Relation with curve severity

No significant, linear correlation could be found between vertebral body or pedicle asymmetry and the Cobb angle or apical vertebral rotation (p > .05; Table 3).

Reliability

In absolute values, the mean intra- and interobserver measurement errors for vertebral body asymmetry measurement were 0.5% and 1.1%, respectively. Since the range of vertebral body asymmetry was relatively small, ICC for intra- and interobserver reliability were relatively low: 0.54 (95% confidence interval: 0.39–0.66) and 0.54 (0.39–0.66), respectively. ICCs for intra- and interobserver reliabilities for pedicle width were 0.98 (0.97–0.98) and 0.97 (0.96–0.97), for pedicle length 0.83 (0.78–0.86) and 0.60 (0.50–0.68), for ideal screw trajectory length 0.91 (0.89–0.93) and 0.82 (0.77–0.85) and for transverse pedicle angle 0.88 (0.85–0.90) and 0.70 (0.63–0.76), respectively.

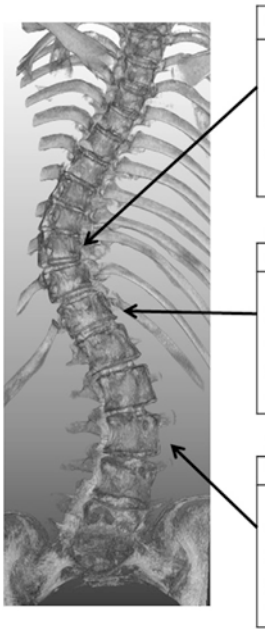

Thoracic apex

Vertebral body asymmetry (%) *	95.8±1.5		
	Concave	Convex	P
Pedicle width (mm) *	4.5±1.2	5.4±1.2	<0.001
Pedicle length (mm) *	20.9±3.5	17.9±2.3	<0.001
Pedicle screw trajectory length (mm) *	43.0±5.2	37.3±4.3	<0.001
Transverse pedicle angle (°) *	12.3±6.4	5.7±3.8	<0.001

Cobb end vertebra

	Thoracic			Lumbar		
Vertebral body asymmetry (%)	96.3±1.0			95.4±1.2		
	Concave	Convex	P	Concave	Convex	P
Pedicle width (mm)	6.9±1.5	6.7±1.3	0.207	6.2±1.3	6.9±1.6	0.040
Pedicle length (mm)	21.4±3.6	20.9±3.8	0.126	20.0±2.9	22.3±3.7	0.003
Pedicle screw trajectory length (mm)	42.2±6.3	40.2±6.9	<0.001	40.3±5.9	42.3±5.2	0.125
Transverse pedicle angle (°)	9.3±6.1	7.6±6.7	0.070	11.6±8.2	6.1±4.2	0.014

Lumbar apex

Vertebral body asymmetry (%)	95.5±1.9		
	Concave	Convex	P
Pedicle width (mm)	5.1±1.4	5.6±2.0	0.212
Pedicle length (mm)	21.9±1.3	24.5±1.9	<0.001
Pedicle screw trajectory length (mm)	45.5±4.3	46.7±4.1	0.182
Transverse pedicle angle (°)	16.5±8.1	9.5±4.6	0.015

Fig. 6. The vertebral asymmetry and pedicle asymmetry are shown for the thoracic apex, Cobb end vertebra and lumbar apex of the primary curves in adolescent idiopathic scoliosis (AIS). *Significant difference between the thoracic or lumbar apex *and* the Cobb end vertebra for vertebral asymmetry and pedicle asymmetry (difference between convex and concave).

Table 3
The Pearson correlation coefficient (r) between the asymmetry parameters in the apical vertebra of the primary curves in the transverse plane versus axial rotation in the corresponding vertebra and the Cobb angle of the curvature.

Correlation	Thoracic				Lumbar			
	Apical vertebral rotation		Cobb angle		Apical vertebral rotation		Cobb angle	
	r	p	r	p	r	p	r	p
Vertebral body asymmetry	0.16	.21	−0.23	.07	−0.34	.21	−0.41	.14
Pedicle width asymmetry	−0.08	.56	0.03	.80	0.54	.04	0.16	.57
Pedicle length asymmetry	0.06	.65	−0.11	.41	0.44	.10	0.40	.14
Ideal pedicle screw trajectory length asymmetry	−0.01	.92	−0.41	.75	0.40	.14	−0.4	.88
Transverse pedicle angle	−0.94	.47	−0.13	.31	0.15	.59	−0.31	.26

Discussion

Accurate descriptions of the 3-D deformity in scoliosis were already given by 19th-century anatomists in cadaveric specimen [1-3]. More recently, with modern imaging techniques, asymmetry in pedicle dimensions between the convex and concave sides of the curve were demonstrated in several studies [8,10-13,22]. The role of this asymmetry, and whether it represents an active asymmetrical growth pattern, or a passive adaptation due to asymmetrical biomechanical loading as explained by Hueter-Volkmann's and Wolff's law, remains undetermined so far [14,15,23,24]. Experimental studies have shown that asymmetrical growth of the NCJs of the vertebrae can lead to vertebral rotation; unilateral lag screw epiphysiodesis of the NCJ in a growing pig was shown to lead to a rotational, 3-D deformity, similar to AIS [25-27]. If, however, asymmetrical growth of the NCJs (either active or passive) leads to asymmetrical pedicle development in AIS, it implicates that the deformity must already begin to develop before closure of these growth plates, in other words, well before the adolescent growth spurt, when all NCJs have been reported to be closed [9,27,28]. Accurate descriptions of vertebral morphology in scoliosis are therefore important, both theoretically, for better understanding its mechanism, and practically, for surgical strategy and safe implant placement.

Our study is, to our knowledge, the first to report asymmetry of both the vertebral bodies and the pedicles, in a population of moderate to severe adolescent idiopathic scoliosis patients, in the true transverse plane, using 3-D multiplanar reconstruction of high-resolution CT scans for each individual vertebra. We used in-house–developed software that has been validated in previous studies, to minimize subjectivity in the measurements [16]. In total, the morphology of 1876 pedicles and 1876 vertebral upper and lower endplates has been accurately assessed for this study in AIS and compared to the same levels in controls. We observed that even in nonscoliotic controls a certain degree of vertebral asymmetry exists. The concave pedicles of the thoracic primary curves were on average 0.4 mm thinner, 1.8 mm longer, the ideal screw trajectory was also on average 4.1 mm longer than for the convex pedicle, and the transverse pedicle angle was 4.6° greater on the concave side. The asymmetry was found to increase toward the apex, the concave pedicle becoming thinner and longer, up to a difference of 0.9 mm thinner and 3.0 mm longer than the convex pedicle. The lumbar concave pedicles were on average 0.5 mm thinner than convex throughout the curve. Although more asymmetry was found in the more rotated apical segments, no direct correlation was found between the amount of asymmetry, the magnitude of the Cobb angle, or the amount of rotation of the apex in these moderate to severe AIS curves. As mentioned in previous studies, the bone drift of the vertebral body toward the concavity and the greater pedicle angle on the concave side explains the longer ideal pedicle screw trajectory on the concave side (Fig. 7) [8].

Our measurements of the pedicle width asymmetry were consistently smaller than the measurements of pedicle width asymmetry that have been reported in previous studies, with a mean difference of 1.0 to 2.4 mm between the convex and concave pedicle [8,22,29-31]. The average asymmetry of the pedicle lengths that have been reported varied between 0.9 and 2.7 mm, the screw trajectory

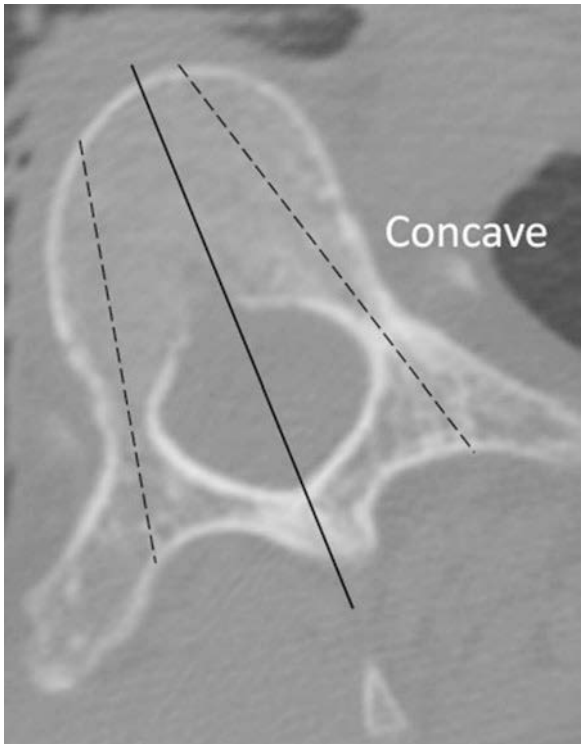

Fig. 7. A thoracic apical vertebral body is shown of a severe curve (Cobb angle 69°). The vertebral body axis (black line) and both the pedicle axes (black dashed lines) are illustrated. The bone drift toward the concavity and the increased transverse pedicle angle causes a longer ideal pedicle screw trajectory.

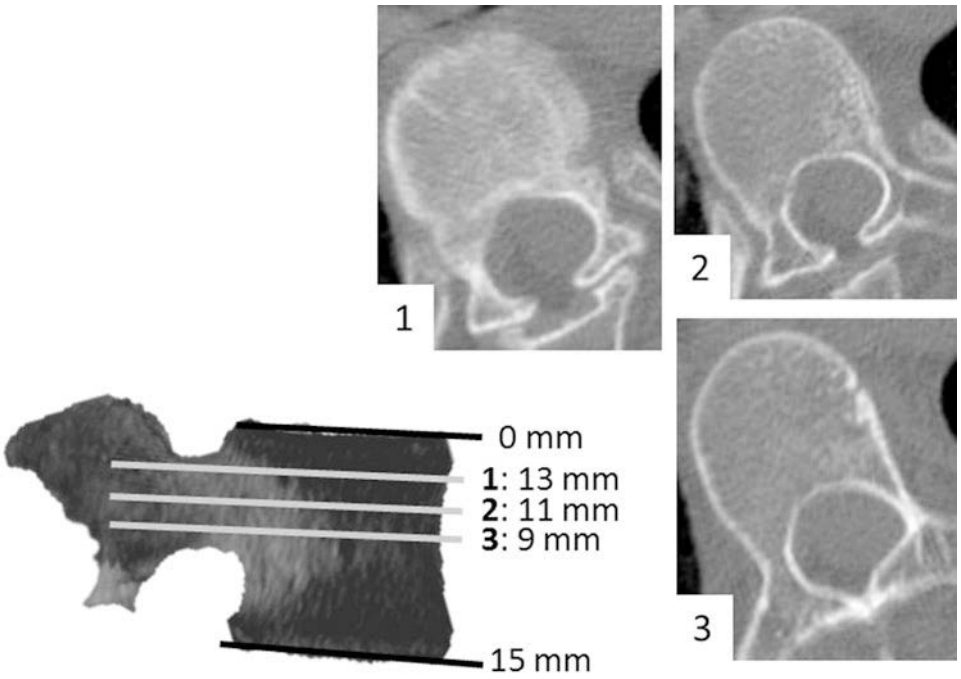

Fig. 8. The measurement method and CT scans should be very accurate; slight deviation from the ideal transverse plane of the rotated, translated, and tilted vertebrae automatically induces apparent, but not necessarily true, asymmetry.

asymmetry between 1.3 and 5.6 mm, and the pedicle angle between 1.3° and 9.0° [8,29-31]. Although CT measurements can be considered the gold standard method for assessment of morphology of in vivo bony structures, it completely depends on voxel size in relation to the size of the structure to be measured. On our high-resolution scan (0.625-mm), we observed that even slight deviations from the ideal transverse plane of the rotated, translated, and tilted vertebrae automatically induces apparent, but not necessarily true, asymmetry (Fig. 8). On the other hand, a major disadvantage of high-resolution CT scans are the radiation dose concerns (the average radiation dose received in this study was 10 mSv), especially for applicability in longitudinal studies.

Unfortunately, this study was conducted in a cross-sectional design. For further understanding of the true nature of the disorder and its etiopathogenesis, future studies need a longitudinal design and modern low-dose or non-ionizing imaging technologies and should focus on mild scoliosis. Nevertheless, this study is a first attempt, because subjects with several curve magnitudes were included and compared to the normal anatomy. Further studies could include a longitudinal design and mild scoliotic patients.

An important issue is how the vertebral body is determined; it depends on where the dividing line between left and right is drawn in these rather irregular structures. Other studies have used varying, sometimes subjective, methods, often based on manually drawing a line by using manually placed points [32]. Our choice of the axis through the vertebral body may be criticized as well. It relies on a manual segmentation of the bony outline of the vertebra, after which the computer determines the center of mass of both the spinal canal and the vertebral body. This creates an objective, very reliable, and reproducible line that divides the vertebra in half, allowing the right half of the vertebra to be ‘‘mirrored’’ to the left half [32]. It also creates some degrees of symmetry, however, because by definition the amount of mass on the left side of this line is identical to the amount of mass on the right side. Although our method will not demonstrate asymmetry in left–right mass distribution, its objectivity and reproducibility, as well as its ability to demonstrate differences in shape between the left and right side of the vertebral body, make it attractive to use [32].

In conclusion, transverse plane vertebral asymmetry exists to a certain extent in normal vertebral bodies and pedicles, but bony asymmetry is more pronounced in AIS, although less than that reported earlier. The less asymmetry as described before is relevant for the pedicle screw size and orientation during the surgical treatment. Vertebral bodies were more asymmetrical in primary lumbar AIS than in primary thoracic curves. Pedicles, however, were more asymmetrical in the apical region of the thoracic curve, the concave pedicle being smaller and longer and the transverse pedicle angle greater than on the convex side. Although curves with greater Cobb angles and more rotation show most vertebral asymmetry, there was no linear correlation between the asymmetry and the amount of rotation in these moderate to severe AIS patients. This suggests to us that asymmetrical vertebral growth does not drive rotation, but rather follows it to a variable extent.

Key points

- This is the first quantitative study on adolescent idiopathic scoliosis describing vertebral body asymmetry as well as pedicle asymmetry in the true transverse plane of each vertebra.
- Vertebral bodies and pedicles were significantly more asymmetrical in AIS than in normal controls. This asymmetry was most pronounced at the thoracic apical vertebrae.
- Although the rotated apical vertebrae showed more asymmetry than the neutral and end vertebrae as well as the same levels in controls, there was no linear relation between the true transverse plane asymmetry and the amount of axial rotation in these moderate to severe AIS patients.

References

[1] Adams W. *Lateral curvature of the spine, external characters and morbid anatomy (lecture 4). Lectures on the pathology and treatment of lateral and other forms of curvature of the spine*. London: Churchill; 1882. p. 69–93.

[2] Albert E. Zur anatomie der skoliose. *Wiener klinische Rundschau* 1895;33:513–5.

[3] Nicoladoni C. Anatomie und mechanismus der skoliose. In: Kocher ET, König FJ, von Mikulicz J, editors. *Bibliotheca medica*. Stuttgart, Germany: Verlag von erwin nagele; 1904.

[4] Von Meyer H. Die mechanik der skoliose. Ein beitrag zur lehre von den missgestaltungen des knochengerüstes. *Virchows Arch* 1866;2:225–53.

[5] Somerville EW. Rotational lordosis; the development of single curve. *J Bone Joint Surg Br* 1952;34-B:421–7.

[6] Roaf R. The basic anatomy of scoliosis. *J Bone Joint Surg Br* 1966;48:786–92.

[7] Schlosser TP, van Stralen M, Brink RC, et al. Three-dimensional characterization of torsion and asymmetry of the intervertebral discs versus vertebral bodies in adolescent idiopathic scoliosis. *Spine (Phila Pa 1976)* 2014;39:E1159–66.

[8] Liljenqvist UR, Link TM, Halm HF. Morphometric analysis of thoracic and lumbar vertebrae in idiopathic scoliosis. *Spine (Phila Pa 1976)* 2000;25:1247–53.

[9] Schlosser TP, Vincken KL, Attrach H, et al. Quantitative analysis of the closure pattern of the neurocentral junction as related to preexistent rotation in the normal immature spine. *Spine J* 2013;13:756–63.

[10] Parent S, Labelle H, Skalli W, et al. Thoracic pedicle morphometry in vertebrae from scoliotic spines. *Spine (Phila Pa 1976)* 2004;29:239–48.

[11] Chu WC, Yeung HY, Chau WW, et al. Changes in vertebral neural arch morphometry and functional tethering of spinal cord in adolescent idiopathic scoliosis—study with multi-planar reformat magnetic resonance imaging. *Stud Health Technol Inform* 2006;123:27–33.

[12] Rajwani T, Bagnall KM, Lambert R, et al. Using magnetic resonance imaging to characterize pedicle asymmetry in both normal patients and patients with adolescent idiopathic scoliosis. *Spine (Phila Pa 1976)* 2004;29:E145–52.

[13] Sarwahi V, Sugarman EP, Wollowick AL, et al. Prevalence, distribution, and surgical relevance of abnormal pedicles in spines with adolescent idiopathic scoliosis vs. no deformity: a CT-based study. *J Bone Joint Surg Am* 2014;96:e92.

[14] Beguiristain JL, De Salis J, Oriaifo A, Canadell J. Experimental scoliosis by epiphysiodesis in pigs. *Int Orthop* 1980;3:317–21.

[15] Canadell J, Beguiristain JL, Gonzalez Iturri J, et al. Some aspects of experimental scoliosis. *Arch Orthop Trauma Surg* 1978;93:75–85.

[16] Kouwenhoven JW, Vincken KL, Bartels LW, et al. Analysis of preexistent vertebral rotation in the normal spine. *Spine (Phila Pa 1976)* 2006;31:1467–72.

[17] Cui G, Watanabe K, Hosogane N, et al. Morphologic evaluation of the thoracic vertebrae for safe free-hand pedicle screw placement in adolescent idiopathic scoliosis: a CT-based anatomical study. *Surg Radiol Anat* 2012;34:209–16.

[18] Watanabe K, Lenke LG, Matsumoto M, et al. A novel pedicle channel classification describing osseous anatomy: How many thoracic scoliotic pedicles have cancellous channels? *Spine (Phila Pa 1976)* 2010;35:1836–42.

[19] Lenke LG, Edwards 2nd CC, Bridwell KH. The Lenke classification of adolescent idiopathic scoliosis: how it organizes curve patterns as a template to perform selective fusions of the spine. *Spine (Phila Pa 1976)* 2003;28:S199–207.

[20] Cobb J. Outline for the study of scoliosis. In: *Instructional Course Lectures*. 2nd ed., 5. The American Academy of Orthopaedic Surgeons, Ann Arbor; 1948. p. 261.

[21] Risser JC. The iliac apophysis: an invaluable sign in the management of scoliosis. *Clin Orthop* 1958;11:111–9.

[22] Abul-Kasim K, Ohlin A. Patients with adolescent idiopathic scoliosis of Lenke type-1 curve exhibit specific pedicle width pattern. *Eur Spine J* 2012;21:57–63.

[23] Volkmann R. Beiträge zur anatomie und chirurgie der geschwülste. *Langenbecks Arch Chir* 1873;15:556–61.

[24] Hueter C. Anatomische studien an den extremitätengelenken neugeborener und erwachsener. *Virchows Arch* 1862;26:484–519.

[25] Roaf R. Vertebral growth and its mechanical control. *J Bone Joint Surg Br* 1960;42-B:40–59.

[26] Knutsson F. A contribution to the discussion of the biological cause of idiopathic scoliosis. *Acta Orthop Scand* 1963;33:98–104.

[27] Taylor JR. Scoliosis and growth. patterns of asymmetry in normal vertebral growth. *Acta Orthop Scand* 1983;54:596–602.

[28] Rajwani T, Bhargava R, Moreau M, et al. MRI characteristics of the neurocentral synchondrosis. *Pediatr Radiol* 2002;32:811–6.

[29] Takeshita K, Maruyama T, Chikuda H, et al. Diameter, length, and direction of pedicle screws for scoliotic spine: analysis by multiplanar reconstruction of computed tomography. *Spine (Phila Pa 1976)* 2009;34(8):798–803.

[30] Upendra B, Meena D, Kandwal P, et al. Pedicle morphometry in patients with adolescent idiopathic scoliosis. *Indian J Orthop* 2010;44:169–76.

[31] Kuraishi S, Takahashi J, Hirabayashi H, et al. Pedicle morphology using computed tomography-based navigation system in adolescent idiopathic scoliosis. *J Spinal Disord Tech* 2013;26:22–8.

[32] Vrtovec T, Pernus F, Likar B. A review of methods for quantitative evaluation of axial vertebral rotation. *Eur Spine J* 2009;18:1079–90.